

# Estimation of Current Distribution on Multilayer Printed Circuit Board by Near-Field Measurement

Qiang Chen, *Member, IEEE*, Sumito Kato, and Kunio Sawaya, *Senior Member, IEEE*

**Abstract**—A method of estimating the current distribution on a microstrip transmission line of a multilayer printed circuit board (PCB) by measuring the near-field distribution is proposed. The microstrip transmission line on the PCB is divided into electrically small segments. An electric field integral equation (EFIE) is established to relate the near field to the current on these segments. The current is estimated by measuring the near field, evaluating the mutual impedance between the current segments, and solving the EFIE. The measurement parameters for near-field measurement are optimized by numerical analysis. Experimental results are presented and compared with the numerical results, confirming the validity of this method.

**Index Terms**—Current distribution, measurement, microstrip line, near-field, printed circuit board (PCB).

## I. INTRODUCTION

THE PROBLEM of electromagnetic interference between electrical circuits and devices is becoming more and more serious because the clock frequency of the electrical circuits is increasing rapidly, and high-density packaging and multilayer printed circuit board (PCB) technologies are widely applied to PCB design. When a problem occurs in an electrical device, it is necessary to know in advance the electric current distribution on the PCB of the electrical device in order to identify the location where the undesired electromagnetic wave is being radiated. Based on the estimated current distribution, the PCB design can be revised to reduce the effects of interference.

The current distribution on the PCB can be measured directly by using a magnetic probe such as a small loop antenna. However, it is difficult to estimate the current distribution on a multilayer PCB because the measured magnetic field is produced by not only the current flowing on the top layer but also that on other layers below the probe. Therefore, it is necessary to distinguish the radiation caused by the currents on different layers.

In previous related research, the equivalent source approach has been studied [1]–[7]. This approach was originally used to calculate the radiation from aperture antennas, which are replaced by the equivalent magnetic current located at equally

spaced meshes of a two-dimensional plane in [1]–[3]. The electric current was also used as the equivalent source instead of the equivalent magnetic current to solve the radiation problem of aperture sources [4], [5]. In these studies, a coupling equation was established between the electric field radiated by the equivalent currents and the value of the equivalent currents by using the free space Green's function. The value of equivalent current was evaluated by measuring the near electric field and solving the coupling equation. A uniform wire-mesh composed of magnetic dipoles was used as an equivalent source to investigate the radiation of small printed antennas [6], and the method was then improved by using a Tikhonov regularization technique [7]. The near field radiated by the magnetic dipoles was evaluated analytically, and the current distribution on the wire mesh was obtained by measuring the near magnetic field and solving the analytical equation. The method utilizing the equivalent source is effective in evaluating the far field by measuring the near-field distribution of a radiation source. However, although the current of the equivalent source can be evaluated, the real current distribution on the radiator is still unknown.

The objective of the present study is to estimate the real current distribution on a multilayer PCB at high frequency. The PCB is assumed to be composed of microstrip transmission lines and lumped circuit elements. The current on the microstrip line is divided into electric current segments with unknown magnitudes and phases. Because of the presence of the dielectric substrates and complicated structure of the microstrip lines, the coupling equation between the radiated field and the expanded electric currents is evaluated by the finite-difference time-domain (FDTD) method, which is an effective full-model analysis method for easily modeling various configurations of the PCB. The unknown current segments are evaluated by measuring the near field and calculating the coupling equation.

To our knowledge, there have been no previous reports of estimating the current distribution on a PCB, especially a multilayer PCB, being by near-field measurement. Some reports described approaches to estimating the "equivalent current" on printed antennas, but the approaches and obtained results were different from the present method. A full-wave analysis of FDTD including the PCB boundary condition is used in this approach to link the measured field and the real current distribution, instead of the Green's function in free space to link the measured field and the equivalent current in the previous studies. This paper presents the measurement parameters and estimation models to show how to choose the probe length and measurement distance, which are dependent on the cell size of the FDTD analysis, because estimation of the real current distribution requires more accurate near-field measurement than the equivalent current

Manuscript received July 13, 2007; revised August 25, 2007. This work was supported in part by the Ministry of Education, Science, Sports and Culture under Grant-in-Aid for Scientific Research (A) 17206039, 2005.

Q. Chen and K. Sawaya are with the Department of Electrical and Communication Engineering, Tohoku University, Sendai 980-77, Japan (e-mail: chenq@ecei.tohoku.ac.jp; sawaya@ecei.tohoku.ac.jp).

S. Kato is with the KDDI Corporation, Chiyoda-ku, Tokyo 102-8460, Japan, and was also with Department of Electrical and Communication Engineering, Tohoku University, Sendai 980-77, Japan (e-mail: sumito@ecei.tohoku.ac.jp).

Color versions of one or more of the figures in this paper are available online at <http://ieeexplore.ieee.org>.

Digital Object Identifier 10.1109/TEMC.2008.921028

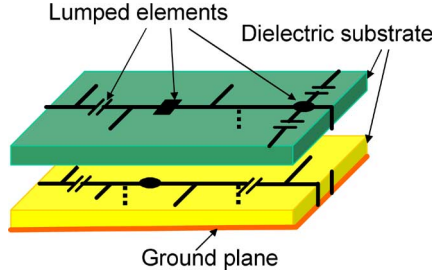


Fig. 1. Multilayer PCB.

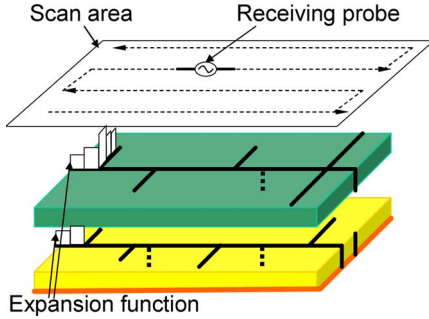


Fig. 2. Expansion of current on microstrip transmission line and scan area of near-field measurement.

estimation for far-field evaluation. It also demonstrates how to deal with the lumped circuits in a PCB whose electrical parameters are assumed to be unknown. First, the approach used to estimate the current distribution on a multilayer PCB by measuring the near field is described. Then, the optimum parameters for the near-field measurement, such as the measurement position, the area of the scanning plane, and the number of measuring points, are discussed by introducing the condition number of the impedance matrix and performing numerical simulations. Finally, experimental estimation results are presented to demonstrate the validity of the method.

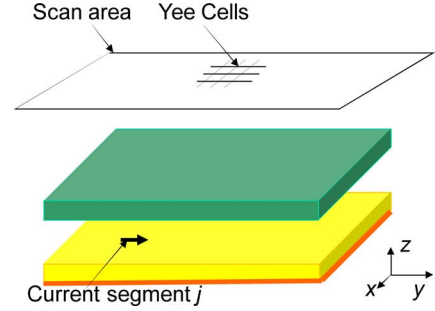
## II. APPROACH

Let us consider the general case of a multilayer PCB, as shown in Fig. 1, which has two layers and some lumped elements implemented on the microstrip transmission line. The objective is to estimate the current flowing on the transmission line on both the top layer and the middle layer.

The model of the multilayer PCB for current estimation is shown in Fig. 2. All the lumped elements have been removed because they do not radiate electromagnetic fields. The microstrip transmission line is divided into current segments that are electrically small. When the current on each segment has a distribution  $\mathbf{f}_j(r)$ , the current distribution on the transmission line is expanded in terms of the expansion function as

$$\mathbf{I}(\mathbf{r}) = \sum_{j=1}^N I_j \mathbf{f}_j(\mathbf{r}) \quad (1)$$

where  $I_j$  is the unknown coefficient to be evaluated,  $N$  is the total number of divided segments, and the expansion function

Fig. 3. FDTD analysis model for evaluating tangential electric field on probe scan area radiated by current segment  $i$ .

$\mathbf{f}_j(r)$  is a pulse function, expressed as

$$\mathbf{f}_j(\mathbf{r}) = \begin{cases} 1, & \mathbf{r} \in \text{segment } j \\ 0, & \text{otherwise.} \end{cases} \quad (2)$$

The electric field integral equation (EFIE)

$$\mathbf{E}(\mathbf{r}) = \int \bar{\mathbf{G}}(\mathbf{r}, \mathbf{r}') \cdot \mathbf{I}(\mathbf{r}') d\mathbf{r}' \quad (3)$$

is introduced to relate the electric near field  $\mathbf{E}(\mathbf{r})$  to the current  $\mathbf{I}(\mathbf{r})$  on these segments, where  $\bar{\mathbf{G}}(\mathbf{r}, \mathbf{r}')$  is the dyadic Green's function satisfying the boundary condition of the multilayer substrate. If the electric near field is measured, the current can be evaluated when the Green's function is known. The integral equation (3) can be changed into linear equations as

$$V_i = \sum_{j=1}^N Z_{ij} I_j, \quad i = 1 - M \quad (4)$$

by combining (1)–(3), where  $Z_{ij}$  is the mutual impedance between the  $j$ th current segment  $\mathbf{f}_j$  and the probe at the  $i$ th position, which is evaluated numerically,  $V_i$  is the voltage received by the probe at each measuring point  $i$ , and  $M$  is the number of measuring points.

Because the PCB is usually composed of a dielectric substrate with a complicated structure in practice,  $Z_{ij}$  cannot be expressed in a closed form. In this research,  $Z_{ij}$  was evaluated numerically using the FDTD method. The model used for FDTD analysis is shown in Fig. 3. For a current segment  $i$  having a distribution  $\mathbf{f}_j$  with a unit coefficient, the radiated tangential components of the electric field at the Yee cells inside the scan area where the near field is measured by the probe are calculated and stored in advance. The FDTD calculation is performed  $N$  times until the radiated field on the scan area for all the current segments are obtained. If a thin-wire dipole is used as the probe for the electric near-field measurement, the impedance matrix in (4) is evaluated by

$$Z_{ij} = \frac{1}{I_j} \sum_{k=1}^K \int \mathbf{E}_k(\mathbf{r}) \cdot \mathbf{w}_i(\mathbf{r}) d\mathbf{r} \quad (5)$$

in the sense of the reaction between the dipole probe at position  $i$  and the current segment  $j$ , where  $\mathbf{w}_i(r)$  is a piecewise sinusoidal function expressing the current distribution on the dipole probe, and  $K$  is the number of Yee cells included in the dipole surface,

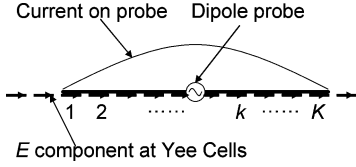


Fig. 4. Positions of probe and Yee cells in FDTD analysis.

and the integration is carried out along the thin-wire dipole. The positions of the probe and Yee cells in the FDTD analysis are shown in Fig. 4.

Because  $V_i$  is obtained by measurement and  $Z_{ij}$  is calculated, the unknown current coefficients  $I_j$  can be obtained by solving (4), which is expressed in a matrix equation form as

$$[Z][I] = [V] \quad (6)$$

where  $[Z]$  is an  $M \times N$  impedance matrix,  $[I]$  is an  $N$ -element vector, and  $[V]$  is an  $M$ -element vector. The number of measurement points  $M$  is usually larger than the number of segments  $N$ . Therefore, the matrix equation is solved by using generalized matrix inversion as

$$[I] = ([Z]^H [Z])^{-1} [Z]^H [V], \quad M \geq N \quad (7)$$

where  $[Z]^H$  is the Hermitian conjugate matrix of  $[Z]$ .

The correlation coefficient  $\gamma$  between the estimated and real current distributions is introduced to evaluate the accuracy of the current estimation, which is defined by

$$\gamma = \frac{|\sum_{i=1}^N (I_i - I^*)(\bar{I}_i - \bar{I}^*)|}{\sqrt{\sum_{i=1}^N (I_i - I^*)^2} \sqrt{\sum_{i=1}^N (\bar{I}_i - \bar{I}^*)^2}} \quad (8)$$

where  $[I]$  is the estimated solution given by (7) and  $[\bar{I}]$  is an exact solution. In this research, the exact solution is obtained by using the FDTD simulation.  $I^*$  and  $\bar{I}^*$  are the averages of  $I_i$  and  $\bar{I}_i$ , respectively.

Because the estimated solution is evaluated by generalized matrix inversion, the accuracy of estimation is greatly affected by the numerical stability of the matrix inversion. Therefore, the condition number  $\kappa$  is also introduced to examine the stability, which is defined by

$$\kappa = \frac{\mu_{\max}}{\mu_{\min}} \quad (9)$$

where  $\mu_{\max}$  and  $\mu_{\min}$  are the maximum and minimum eigenvalues of  $[Z]^H [Z]$ . A large value of  $\kappa$  means that the solution  $[I]$  is sensitive to the error in  $[V]$  due to the near-field measurement.

### III. OPTIMIZATION OF MEASUREMENT PARAMETERS

We used numerical simulation to determine the measurement parameters such as the near-field measurement points, the scanning plane area, the distance between the PCB surface and the scanning plane, and the length of the receiving probe. The near field was obtained by numerical simulation by FDTD instead of by measurement. In the FDTD simulation, an absorbing boundary condition of the Mur second order was applied and the Yee cell size could be changed within the range from 2.5 to 5 mm. A sinusoidal time-varying voltage was excited continuously over

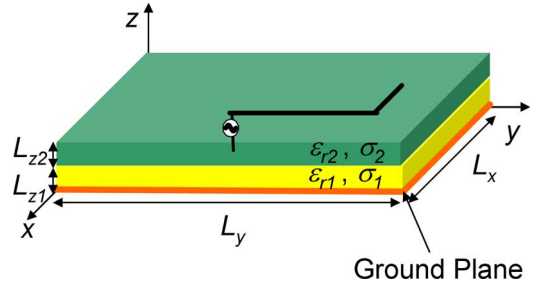


Fig. 5. Two-layer PCB for current estimation experiment.

 TABLE I  
 CONFIGURATION OF DIELECTRIC SUBSTRATE OF  
 TWO-LAYER PCB SHOWN IN FIG. 5

frequency [GHz]	1.5
$L_x, L_y, L_{z1}, L_{z2}$ [ $\lambda$ ]	0.6, 0.6, 0.008, 0.008
$\epsilon_{r1}, \epsilon_{r2}$	4.4, 4.4
$\sigma_1, \sigma_2$ [S/m]	$2.13 \times 10^{-3}, 2.13 \times 10^{-3}$

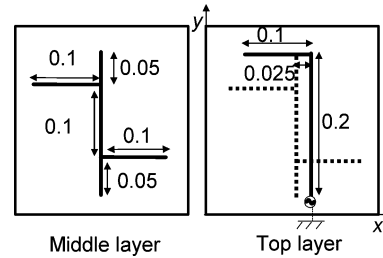


Fig. 6. Geometry of microstrip line on each layer of the two-layer PCB shown in Fig. 5.

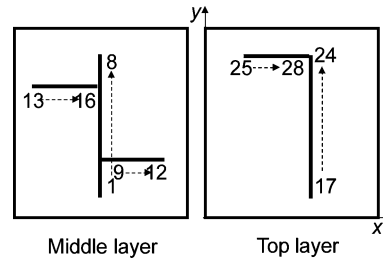


Fig. 7. Number of current segments on microstrip line of the two-layer PCB shown in Fig. 5.

a one-cell gap at the feed point. The FDTD region was divided into up to  $120 \times 120 \times 200$  Yee cells when the cell size was 2.5 mm. Gaussian noise, which appeared in the measurement, was added to the received voltage to maintain the SNR level in the simulation. Let us consider a two-layer PCB as the model for current estimation. Its geometry is shown in Fig. 5 and Table I. The layout of the microstrip configuration on each layer is shown in Fig. 6. The location numbers of the current segments on the microstrip line are shown in Fig. 7. Current segments from 1 to 16 correspond to the current on the microstrip line of the middle layer. Segments from 17 to 28 correspond to that of the top layer. The microstrip line is excited by a 1.5-GHz continuous wave at the gap between the ground and segment 17 on the top layer, while the microstrip line on the middle layer is not fed directly but is electrically coupled by the top layer. Of

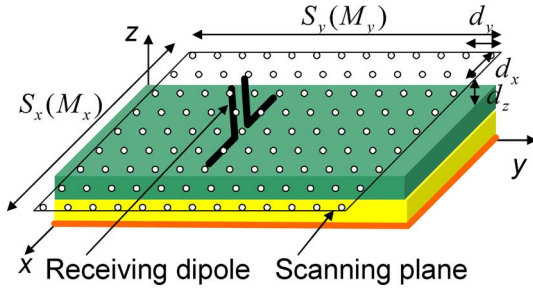


Fig. 8. Geometry of scanning plane for measuring the near field above the PCB.

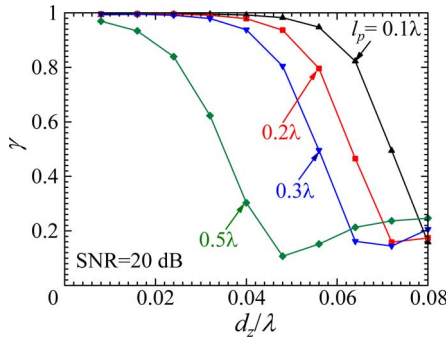


Fig. 9. Correlation coefficient  $\gamma$  as a function of distance  $d_z$  and dipole length  $l_p$ .

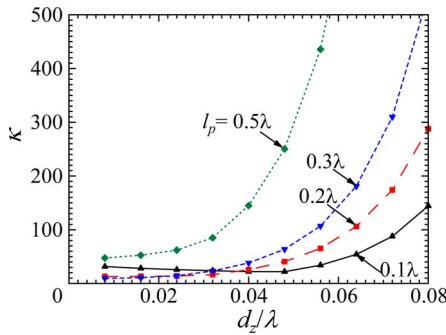


Fig. 10. Correlation coefficient  $\gamma$  and condition number  $\kappa$  as a function of distance  $d_z$ .

course, the feed position is assumed to be an unknown factor in the estimation procedure.

The scanning plane for the near-field measurement is shown in Fig. 8. The dipole probe has a total length of  $2l_p$ . The distance between the source model, and scanning plane is  $d_z$ . The scanning plane has an area of  $S_x \times S_y$  corresponding to  $M_x \times M_y$  sampling points. The intervals of the measuring points are  $d_x$  and  $d_y$  in the  $x$ - and  $y$ -directions, respectively.

Fig. 9 shows the correlation coefficient  $\gamma$  as a function of distance  $d_z$  and dipole length  $l_p$ , when  $S_x = S_y = 0.3 \lambda$  and SNR = 20 dB. We found that a smaller probe and a smaller distance resulted in more accurate current estimation. For example, if the probe has a length of  $0.2 \lambda$ , then distance  $d_z$  should be less than  $0.06 \lambda$  to keep the correlation coefficient larger than 0.8. The condition number  $\kappa$  in the same condition is shown in Fig. 10.

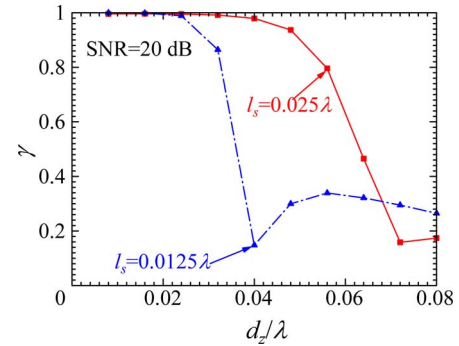


Fig. 11. Correlation coefficient  $\gamma$  versus measurement distance  $d_z$  as a function of segment length  $l_s$ .

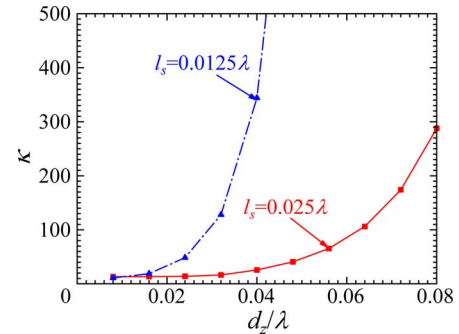


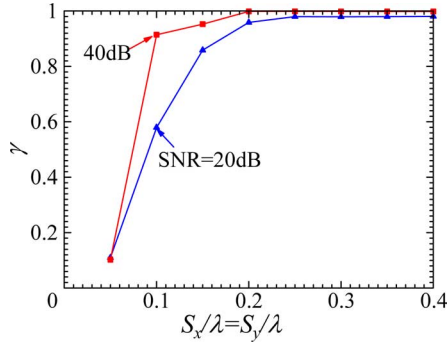
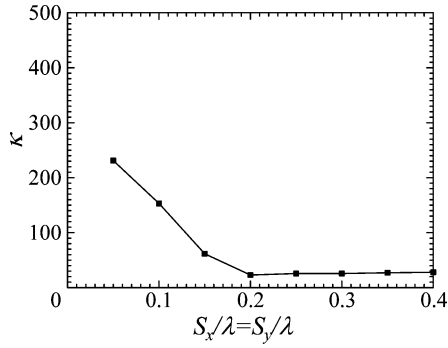
Fig. 12. Condition number  $\kappa$  versus measurement distance  $d_z$  as a function of segment length  $l_s$ .

We found that a smaller probe and a smaller distance led to a smaller condition number.

We performed many simulations for different models and found that the probe length and measurement distance that are suitable for near-field measurement with high accuracy are frequency dependent and that they should be less than 0.3 and 0.1 wavelengths, respectively, in most cases when the SNR is assumed to be 20 dB. For example, if the dipole probe has a length of 3 cm, it can be used at frequencies less than 3 GHz and the measurement distance should be less than 1 cm. On the other hand, because FDTD is used in calculating the mutual coupling between the probe and the PCB and the Yee cell size is probably small due to the complex structure of the PCB, the present method is not suitable for low frequencies. Therefore, it can be said that the low-frequency limitation is determined by the computational ability of the computer used for the FDTD analysis, and the high-frequency limitation is mainly determined by the probe length.

The effects of the length of unknown segments on the measurement accuracy and the stability of the matrix inversion are shown in Figs. 11 and 12, respectively. We found that the more finely the microstrip transmission line is divided, the smaller the distance between the probe and the PCB should be to maintain the measurement accuracy. It seems that the probe distance is strongly determined by the length of the current segments, and a high resolution in current estimation requires a small probe distance.

The effects of the scanning area on the correlation coefficient  $\gamma$  and condition number  $\kappa$  are shown in Figs. 13 and 14,

Fig. 13. Correlation coefficient  $\gamma$  as a function of measuring area  $S_x$  and  $S_y$ .Fig. 14. Condition number  $\kappa$  as a function of measuring area  $S_x$  and  $S_y$ .

respectively, when  $d_z = 0.04 \lambda$  and  $l_p = 0.2 \lambda$ . We found that  $\gamma$  approaches 1 and  $\kappa$  decreases to a constant value when  $S_x$  and  $S_y$  are larger than  $0.2 \lambda$ . This microstrip line is distributed inside the area of  $0.2 \lambda \times 0.2 \lambda$ . This indicates that the near-field scanning should cover the microstrip line where the current is estimated.

In the earlier simulation results, both the coefficient  $\gamma$  and the condition number  $\kappa$  were given in the same cases. We found that the variation of these two parameters has a very strong correlation. For example, in Figs. 9 and 10, if a correlation coefficient larger than 0.8 is required, the measurement parameters should be determined so that the condition number  $\kappa$  is lower than about 50. Since the value  $\kappa$  can be calculated before measuring the near field and evaluating (7), it is a useful and convenient parameter for determining the measurement parameters and predicting the accuracy of the estimation before the near-field measurement.

#### IV. RESULTS OF CURRENT ESTIMATION BY EXPERIMENT

The current distribution on the two-layer PCB shown in Fig. 5 was estimated by using the present method. In the near-field measurement system (shown in Fig. 15), a dipole with an optical modulator was used as the probe shown in Fig. 16. The signal received by the probe was modulated by an optical modulator and transmitted to an optical/electrical demodulator through an optical fiber instead of through a radio-frequency cable to reduce the interference with the measured current distribution. The dipole probe was moved by a planar scanner at a constant distance  $d_z$  between the probe and surface of the measured PCB. A network analyzer was used to feed the measured PCB

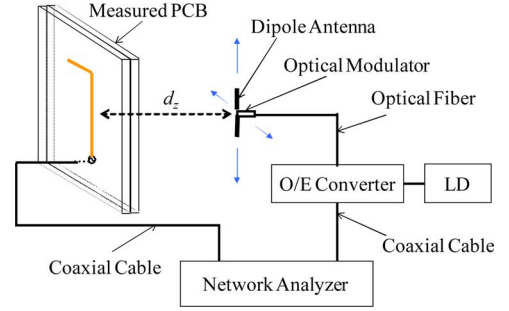


Fig. 15. Near-field measurement system.

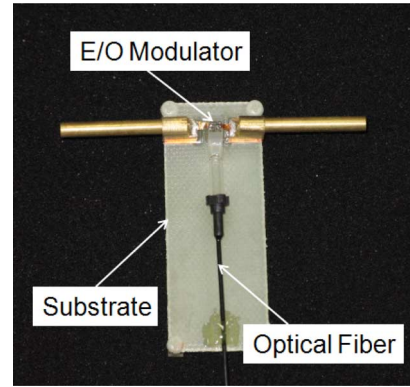


Fig. 16. Dipole antenna with optical modulator as near-field probe.

TABLE II  
MEASUREMENT PARAMETERS FOR PCB CURRENT ESTIMATION

$L_x, L_y$ [ $\lambda$ ]	0.3, 0.3
$M_x, M_y$	13, 13
$l_p$ [ $\lambda$ ]	0.2
$l_s$ [ $\lambda$ ]	0.025
$d_z$ [ $\lambda$ ]	0.025

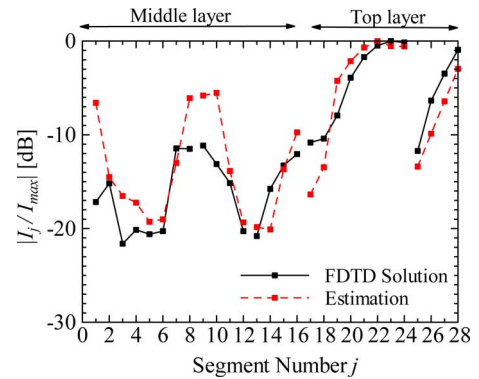


Fig. 17. Estimated current distribution on microstrip line in Fig. 6 compared with FDTD solution.

and the signal received from the dipole probe. The measurement parameters are shown in Table II.

The relative magnitude of the estimated current distribution is shown in Fig. 17. The FDTD solution of the current distribution is also plotted for comparison, where the feed point is given in the FDTD simulation. Some discrepancies can be seen between the estimated and simulated results in Fig. 17. There

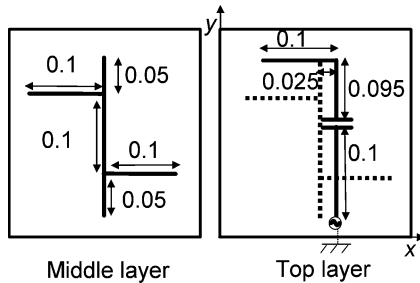


Fig. 18. Geometry of microstrip line on each layer of the two-layer PCB with a lumped capacitor.

are two main reasons for errors in the present method. One is the difference between the practical model and estimation model. In the estimation model, the feed point is not included because it is assumed to be unknown. Therefore, the estimated current in the segments near the feed point (segments 1, 2, 17, and 18) may have a relatively large error. The other reason is the limited dynamic range of the receiving probe used in the measurement. Because the current on the middle layer is excited by electromagnetic coupling from the top layer, the amplitude of the current is much smaller than that of the current on the top layer. Furthermore, because the probe was scanned on the surface of the top layer, the electromagnetic coupling between the current on the middle layer and the receiving probe was relatively weak. Therefore, the accuracy of the estimated current on the middle layer suffered from measurement error more easily than that on the top layer. This reason can explain the discrepancies between estimated and simulated results for segments from 1 to 16 on the middle layer. However, this error was caused by measurement error, not by the measurement method. Therefore, the error can be reduced by improving the accuracy of the near-field measurement, for example, by using a network analyzer with a lower noise level, and an optical modulator and a demodulator with higher sensitivity.

To demonstrate the accuracy of the present method in dealing with lumped electric elements, we included a capacitor in the transmission line of the earlier PCB model. Fig. 18 shows the geometry of the microstrip line of the PCB model, where there is a slit with a width of 1 mm at segment 21 in the microstrip line on the top layer. The narrow slit can be considered to be a lumped capacitor. The near field was measured on the surface of the model, while the estimation model was the same as shown in Fig. 7, where the capacitor is not included. The relative magnitude of the estimated current distribution of the model is shown in Fig. 19. Because the lumped circuits are not considered in the estimation model, the estimated current in the lumped circuit element (segment 21) is not correct. However, the accuracy of the estimated current near the segment is little affected by the presence of the lumped circuit, which is neglected in the estimation model. This demonstrates the validity of the present approach for dealing with lumped circuit elements in the estimation model. The present method can be called practicable because it requires only the physical parameters of the PCB, but does not require prior knowledge about the electrical properties of the lumped circuit elements in the circuit board. The

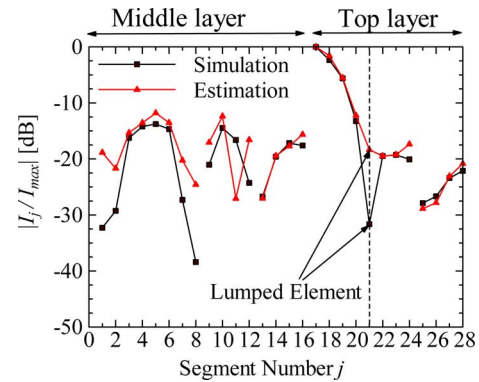


Fig. 19. Estimated current distribution on microstrip line in Fig. 18 compared with FDTD solution.

physical parameters of the PCB are usually known, but the electrical properties of the lumped circuit elements are unknown in practice.

## V. SUMMARY

A method of estimating the current distribution by measuring the near-field distribution has been proposed and applied to estimate the current flowing on microstrip transmission lines on different layers of a multilayer PCB. A guideline has been given to show how to determine the measurement parameters to measure the near field to estimate the current distribution at a given SNR ratio, such as the measurement distance, the scanning plane area, and the probe size. The approach to deal with lumped element circuits has been demonstrated to be valid for a PCB with lumped element circuits whose electrical parameters are known. The current distribution of a two-layer microstrip line with a lumped capacitor has been estimated experimentally, confirming the validity of the method.

## ACKNOWLEDGMENT

Part of this research was performed by M. Hangai, M. Teramoto, and K. Takasu, former graduate students of Tohoku University, Sendai 980-77, Japan.

## REFERENCES

- [1] P. Petre and T. K. Sarkar, "Near-field to far-field transformation using an equivalent magnetic current approach," *IEEE Trans. Antennas Propag.*, vol. 40, no. 11, pp. 1348–1356, Nov. 1992.
- [2] A. Taaghoul and T. K. Sarkar, "Near-field to near/far-field transformation for arbitrary near-field geometry, utilizing an equivalent magnetic current," *IEEE Trans. Electromagn. Compat.*, vol. 38, no. 3, pp. 536–542, Aug. 1996.
- [3] S. Blanch, R. G. Yaccarino, J. Romeu, and Y. Rahmat-Samii, "Near-field to far-field transformation of bi-polar measurements by equivalent magnetic current approach," in *Proc. IEEE AP-S Symp.*, Jun. 1996, pp. 561–564.
- [4] P. Petre and T. K. Sarkar, "Planar near-field to far-field transformation using an array of dipole probes," *IEEE Trans. Antennas Propag.*, vol. 42, no. 4, pp. 534–537, Mar. 1994.
- [5] T. K. Sarkar and A. Taaghoul, "Near-field to near/far-field transformation for arbitrary near-field geometry utilizing an equivalent electric current and MoM," *IEEE Trans. Antennas Propag.*, vol. 47, no. 3, pp. 566–573, Mar. 1999.

- [6] J.-J. Laurin, F.-F. Zürcher, and F. E. Gardiol, "Near-field diagnostics of small printed antennas using the equivalent magnetic current approach," *IEEE Trans. Antennas Propag.*, vol. 49, no. 5, pp. 814–828, May 2001.
- [7] J. Colinas, Y. Goussard, and J.-J. Laurin, "Application of the Tikhonov regularization technique to the equivalent magnetic currents near-field technique," *IEEE Trans. Antennas Propag.*, vol. 52, no. 11, pp. 3122–3132, Nov. 2004.
- [8] Q. Chen, M. Hangai, and K. Sawaya, "Estimation of current distribution by near-field measurement," in *Proc. Asia-Pacific Conf. Environ. Electromagn.*, 2003, pp. 482–484.



**Qiang Chen** (M'97) received the B.E. degree in electrical engineering from Xidian University, Xi'an, China, in 1986, and the M.E. and D.E. degrees in electrical engineering from Tohoku University, Sendai, Japan, in 1991 and 1994, respectively.

He is currently an Associate Professor in the Department of Electrical Communications, Tohoku University. He is now an Associate Editor for the *Transactions of Communications of Institute of Electronics, Information, and Communication Engineers (IEICE)*. His current research interests include computational electromagnetics, adaptive array antennas, and antenna measurement.

Dr. Chen received the Young Scientists Award in 1993 from the IEICE of Japan. He has been the Secretary and a Treasurer of the IEEE Antennas and Propagation Society Japan Chapter in 1998, the Secretary of the Technical Committee on Electromagnetic Compatibility of IEICE from 2004 to 2006, and the Secretary of Tohoku Branch of the Institute of Image Information and Television Engineers of Japan from 2004 to 2007.



**Sumito Kato** was born in Akita, Japan, in 1984. He received the B.E. and M.E. degrees in electrical engineering from Tohoku University, Sendai, Japan, in 2006 and 2008, respectively.

Since April 2008, he has been with KDDI Corporation, Tokyo, Japan.

Mr. Kato is a member of the Institute of Electronics, Information and Communication Engineers of Japan, and a member of the Institute of Image Information and Television Engineers of Japan.



**Kunio Sawaya** (M'79–SM'02) received the B.E., M.E., and D.E. degrees in electrical engineering from Tohoku University, Sendai, Japan, in 1971, 1973, and 1976, respectively.

He is currently a Professor in the Department of Electrical and Communication Engineering, Tohoku University. His current research interests include antennas in plasma, antennas for mobile communications, theory of scattering and diffraction, antennas for plasma heating, and array antennas.

Prof. Sawaya received the Young Scientists Award in 1981 and the Paper Award in 1988 both from the Institute of Electronics, Information and Communication Engineers (IEICE) of Japan. He was the Chairman of the Technical Group of Antennas and Propagation of the IEICE from 2001 to 2003. He is a Fellow of the IEICE and a member of the Institute of Image Information and Television Engineers of Japan.